A Haptic Teleoperation of Agricultural Multi-UAV

Chanyoung Ju, Sungjun Park, Sangsoo Park, and Hyoung Il Son, *Member, IEEE,*

***Abstract*—In this study, we propose a distributed swarm control algorithm for an agricultural multiple unmanned aerial vehicle (UAV) system that enables a single operator to remotely control a multi-UAV system. The system has two control layers that consist of a teleoperation layer through which the operator inputs teleoperation commands via a haptic device and a UAV control layer through which the motion of UAVs is controlled by a distributed swarm control algorithm. In the teleoperation layer, the operator controls the desired velocity of the UAV by manipulating the haptic device and simultaneously receives the haptic feedback. In the UAV control layer, the distributed swarm control consists of the following three control inputs: 1) velocity control , 2) formation control, and 3) collision avoidance control. The three controls are input to each UAV for the distributed system. The proposed algorithm is implemented in the dynamic simulator, and experimental results using four UAVs are presented to evaluate and verify the algorithm.**

Keywords*—agricultural UAV, multi-UAV system, distributed swarm control, haptic teleoperation, UAV simulator.

I. Introduction

When drones or unmanned aerial vehicles (UAVs) are used in agriculture, it is possible to create a map that reconstructs the location of farmland and crops in three dimensions. Subsequently, the yield of crops is estimated through sensors mounted on the UAV [1]. Furthermore, the health index and vegetation index of crops are calculated through visual, infrared, and thermal information measured by the UAV and the method using agricultural UAV more accurately detects pests and diseases that cannot be observed well on the ground and facilitate eco-friendly and high-efficiency agriculture by applying variable amounts of water, fertilizer, and pesticide based on the state of the crop [2]. Thus, agricultural UAVs display excellent potential in addition to low maintenance costs that are used in a variety of farming applications and are growing rapidly as a major technology for agriculture [3].

However, an individual UAV involves limitations in terms of weight, size, and energy consumption for itself as well as for the sensors that it carries [4]. A method to alleviate these problems involves performing farming by using multiple vehicles that cooperate to achieve the mission goal (i.e., crop scouting, seeding, pesticide spraying, and transport). Various improvements occur when a multi-UAV system that can improve robustness is used and include a reduction in the completion time and an increase in the amount of work relative to time when compared to those when a single-UAV system is applied [5]. Therefore, the deployment of multiple UAVs further increases agricultural working efficiency by utilizing the advantages of a multi-UAV system. The application involving multi-UAV systems is used for detecting, localizing, tracking, surveillance, and intercepting [6]. However, in a few cases, the multi-UAV system was applied to agriculture, and several studies continue to progress (e.g., multi-UAV based cooperative remote sensing for real-time water management and irrigation control) [7]. In this study, we propose a swarm control algorithm that is applied to a multi-UAV system for agriculture.

If a multi-UAV system is introduced for agriculture, a more advanced and smarter system is constructed when compared with the current agricultural environment. However, several difficulties persist in the actual application of the agricultural multi-UAV system. Thus, to adapt to the real agricultural environment, we designed a multi-UAV system by considering the following two methods 1) a UAV control method; and 2) a swarm control method. The first method (UAV control method) involves three typical methods to control the UAV, namely a method of autonomous driving by using Simultaneous Localization and Mapping (SLAM), a method of driving on a certain path as specified by the operator, and a method of teleoperation by the operator in real time. Currently, most methods of controlling UAV in agriculture use the second method by using ground station software such as a Mission Planner or QGroundControl. However, this method specifies the path each time, and thus the system becomes more complicated and difficult when the use of the UAVs increases, and it usually uses a centralized controller while attempting to control multi-UAV. Therefore, it is not suitable to use agricultural multiple UAVs. The best method involves performing agricultural tasks with fully automated UAVs. Unfortunately, it is not currently possible to guarantee the safety of using multiple UAVs that automatically avoid obstacles and fly the path by using SLAM or Machine vision (MV) in unstructured, unspecified, and uncertain agricultural environments. In such cases, fully autonomous control of the UAVs is typically impossible, and instead, a teleoperation of their behaviors is desired if not absolutely necessary to impose human intelligence on the task of coping with the forementioned uncertainties[8], [9]. Additionally, when an operator needs more precise or additional work with an agricultural multi-UAV, the use of a system in which a teleoperation command by the operator is entered in a supplementary manner to control the multi-UAV is more advantageous when applied to agricultural work than the use of an incomplete automated UAV system.

In case of teleoperation, efficiency decreases and costs increase when several operators are mobilized to control multiple UAVs. Thus, an efficient system in which multiple

Chanyoung Ju, Sungjun Park, Sangsoo Park, Hyoung Il Son are with the Department of Rural and Biosystems Engineering, Chonnam National University, 77 Yongbong-ro, Buk-gu, Gwangju 61186, Republic of Korea. Corresponding author : Hyoung Il Son, E-mail: hison@jnu.ac.kr, URL: hralab.jnu.ac.kr, Phone: +82-62-530-2152, Fax: +82-62-530-2159.

Manuscript received July 31, 2017; revised August xx, 2017.

UAVs are remotely controlled by a single operator is required [10]. In [7], several operators were mobilized to control an agricultural multi-UAV used for area coverage and remote sensing . Furthermore, the method that is most commonly used in agriculture currently is the 1:1 control method. Nevertheless, the proposed method in the current study corresponds to a 1:N swarm control method in which it is not necessary to mobilize several operators. In the study, we considered a swarm control method involving the agricultural environment. The following three typical methods exist for swarm control: centralized method, decentralized method, and distributed method. The centralized method is a way to handle and control the whole process by a single reader that contains complete information. This method is relatively easy in terms of implementation of the system and management of data. However, the centralized method is not suitable for outdoor environments, such as agriculture, owing to the lack of a direct connection between UAVs. Thus, swarm control is not performed when an error occurs in the leader as well as when an error occurs in only a single UAV [11]. The distributed method is a way to maintain the swarm control system even if a certain leader includes errors because the distributed controller is mounted in each UAV, and this method is the most stable way to cope with unpredictable errors or accidents. Among the three methods, we swarm control agricultural multiple UAVs by using a more stable and flexible decentralized method, and this system copes with the uncertainty in the agricultural environment.

In summary, the method that is currently used is a 1:1 control method for agricultural multi-UAV via several operators and a system that uses swarm control via a single operator does not exist. Therefore, in the present study, we proposed a distributed swarm control for an agricultural multi-UAV system that enables a single operator to remotely control the multi-UAV. The distributed swarm control consists of the following three control inputs: 1) a velocity control of UAV by using an operator's teleoperation command, 2) a formation control to form the desired formation by using an artificial potential field, and 3) a collision avoidance control to avoid obstacles. In a teleoperation, an operator uses a haptic device to control a multi-UAV, and appropriate haptic feedback is given to an operator. Formation control forms a desired formation by using a potential function that is defined as the relative distance between UAVs. Collision avoidance control automatically avoids obstacles via a repulsive potential field defined as the distance between UAVs and Obstacles. The three controls are input to each UAV for the distributed system. In this study, we implemented a multi-UAV system with a distributed swarm control algorithm into a dynamic simulator and subsequently performed experiments to validate and evaluate the algorithm.

The structure of this paper is as follows. Section II introduces the control architecture based on a distributed swarm control algorithm. Section III shows an overall hardware-in-the-loop simulation that includes an experiment setup, an experimental task, and data analysis. Finally, Section IV and Section V show experimental results by using four UAVs and discuss the conclusions of this study , respectively.

II. DISTRIBUTED SWARM TELEOPRATION

A. UAV Dynamics

We consider N quadrotor-type UAVs with 3-DOF Cartesian positions that are denoted by $p_i \in \Re^3$, $i = 1, 2, ..., N$. Flight control of UAVs is derived from the following under-actuated Lagrangian dynamics equation in $SE(3)$ [12]

$$m_i \ddot{p}_i = -\lambda_i R_i e_3 + m_i g e_3 + \delta_i \quad (1)$$

$$J_i \dot{w}_i + S(w_i) J_i w_i = \gamma_i + \zeta_i, \quad \dot{R}_i = R_i S(w_i) \quad (2)$$

where $m_i > 0$ denotes mass, $p_i := [p_1; p_2; \ldots, p_N] \in \Re^{3N}$ denotes the Cartesian center-of-mass position represented in the north-east-down (NED) inertial frame $\{O\} := \{N^O, E^O, D^O\}$, $\lambda_i \in \Re$ denotes thrust control input, $R_i \in SO(3)$ denotes the rotational matrix describing the body-frame $B := \{N^B, E^B, D^B\}$ of UAV w.r.t. to the inertial frame $\{O\}$, g is the gravitation constant, $e_3 = [0, 0, 1]^T$ denotes the basis vector representing the down direction and representing that thrust and gravity act in the D direction, $J_i \in \Re^{3\times3}$ denotes the UAV's inertia matrix w.r.t. the body frame $\{B\}$, $w_i \in \Re^3$ denotes the angular velocity of the UAV relative to the inertial frame $\{O\}$ represented in the body frame $\{B\}$, $\gamma_i \in \Re^3$ denotes the attitude torque control input, $\delta_i, \zeta_i \in \Re^3$ denote the aerodynamic perturbations, and $S(w_i) : \Re^3 \to so(3)$ denotes the skew-symmetric operator defined s.t. for $\alpha, \beta \in \Re^3, S(\alpha)\beta = \alpha \times \beta$. For typical UAV flying, $\delta_i, \zeta_i \approx 0$

B. Distributed Swarm Control

Our goal involves using the distributed method as opposed to the centralized method to simultaneously control the 3-DOF Cartesian position of N UAVs. The distributed swarm control algorithm approaches the following three fundamental requirements: 1) UAV control; 2) formation control; and 3) obstacle avoidance control [8], [13].

First, to describe the manner in which the UAVs are connected via communication to form the $N-$nodes, we define the dynamic undirected *connectivity graph* $\mathcal{G} \triangleq \{\mathcal{V}, \mathcal{E}\}$ by the vertex set $\mathcal{V} \triangleq \{1, 2, \ldots, n\}$, representing the UAVs and the edge set $\mathcal{E} \triangleq \{e_{ij} : i = 1, 2, \ldots, n, j \in \mathcal{N}_i\}$ representing the connectivity among the UAVs, where the dynamic neighbor set $\mathcal{N}_i$ of UAV i is defined as follows:

$$\mathcal{N}_i \triangleq \{j \in \mathcal{V} : \text{UAV } i \text{ receives information from UAV } j, i \neq j\} \quad (3)$$

Subsequently, we implement the following distributed swarm control on each UAV, for the ith UAV,

$$\dot{p}_i(t) := u_i^u + u_i^c + u_i^o \quad (4)$$

where the meaning of the three control inputs $u_i^u \in \Re^3, u_i^c \in \Re^3$ and $u_i^o \in \Re^3$ represents the velocity terms of the UAV.

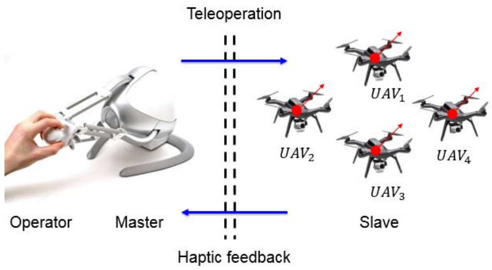

Fig. 1. Concept of a multi-UAV System: haptic teleoperation of multiple UAVs

1) UAV control u_i^u: The UAV control method mainly uses the following three methods: (i)the method of fully autonomous driving, (ii)the method of driving on a certain path specified by the operator, and (iii)the method of teleoperation by the operator in real time (Fig.1). However, as mentioned in Section I, we considered only the method of (iii) given the agricultural environment.

Therefore, we consider a 3-DOF haptic device for master as modeled by the following nonlinear Lagrangian dynamics equation [14]

$$M(q)\ddot{q} + C(q,\dot{q})\dot{q} = \tau + f_h \tag{5}$$

where $q \in \Re^3$ denotes the configuration of the haptic device (e.g., the position of end effector), $M(q) \in \Re^{3\times3}$ denotes the positive-definite/symmetric inertia matrix, $C(q,\dot{q}) \in \Re^{3\times3}$ denotes the Coriolis matrix, and $\tau \in \Re^3$, $f_h \in \Re^3$ denote the control input and human forces, respectively.

The velocity term, $u_i^u \in \Re^3$, represents the teleoperation command for the desired velocity input of the UAV that is directly controlled by the operator by using the configuration of the haptic device q

$$u_i^u = \Lambda q \qquad \forall i \tag{6}$$

where $\Lambda \in \Re^+$ denotes a constant scale factor used to match different scales between q and the UAV desired velocity u_i^u, and $q \in \Re^3$ denotes the position of end effector. In (6), multiple UAVs with an unbounded workspace can fly without the limitations of workspace by controlling the desired velocity by using the configuration of the haptic device with a bounded workspace.

Simultaneously, to allow the operator to telesense a few UAVs and their surrounding obstacles, we consider the haptic feedback $y(t) \in \Re^3$ s.t., as defined by

$$y_f(t) := \frac{1}{\Lambda N}\sum_{i=1}^{N} u_i^o, \quad y_v(t) := q - \frac{1}{\Lambda N}\sum_{i=1}^{N} \dot{x}_i. \tag{7}$$

$$y(t) = y_f + y_v \tag{8}$$

where $\dot{x}_i$ denotes ith UAV's velocity, and u_i^o denotes ith UAV's obstacle avoidance control, $y_f(t)$ denotes force-cue feedback, and $y_v(t)$ denotes velocity-cue feedback. The force-cue feedback plays the role of a repulsive force from the environment. It is related to the difference between the position of UAVs and the location of the obstacles. The velocity-cue feedback represents the difference between the commanded velocity as specified by q and the average velocity of UAVs. This difference is caused due to various reasons and is described in detail in [13]. Finally, $y(t)$ denotes the sum of these two signals y_f and y_v and is sent to the master via the communication channel.

The ultimate objective involves implementing a multi-UAV system that enables a single operator to control N UAVs' Cartesian positions (1) $p := [p_1; p_2; \ldots; p_N] \in \Re^{3N}$ based on the distributed swarm control algorithm via the single 3-DOF haptic device (5) as shown in Fig.1. The operator teleoperates more intuitively by receiving visual feedback as well as haptic feedback based on the information of the N UAV's state and its surrounding environment.

2) Formation control u_i^c: The second velocity term, $u_i^c \in \Re^3$ denotes a control input to avoid a collision among UAVs, preserves connectivity, and achieves a certain desired formation as specified by the desired distances $d_{ij}^c \in \Re^+ \quad \forall i = 1,\ldots,N,$ and $\forall j \in \mathcal{N}_i$, as defined by

$$u_i^c := -\sum_{j\in\mathcal{N}_i} \frac{\partial \varphi_{ij}^c(\|p_i - p_j\|^2)^T}{\partial p_i} \tag{9}$$

where φ_{ij}^c denotes a certain artificial potential function to create an attractive action if $\|p_i - p_j\| > d_{ij}^c$, a repulsive action if $\|p_i - p_j\| < d_{ij}^c$, and a null action if $\|p_i - p_j\| = d_{ij}^c$. The potential function φ_{ij}^c is described in further detail , and φ_{ij}^c consists of V_{ij} and W_{ij} [15]. V_{ij} denotes a repulsive potential function to avoid collision among UAVs and requires the following properties.

1) V_{ij} denotes a function of the square norm of the distance between UAVs i, j, not based on vector
$$V_{ij} = V_{ij}(\|p_i - p_j\|^2) = V_{ij}(\beta_{ij}) \tag{10}$$
2) V_{ij} attains its maximum value whenever $\beta_{ij} \to 0$. In other words, we require that $V_{ij} \to \infty$ whenever $\beta_{ij} \to 0$.
3) It is continuously differentiable from everywhere.
4) $\partial V_{ij}/\partial p_i = 0$ and $V_{ij} = 0$ whenever $\beta_{ij} > (d_{ij}^c)^2$.
5) $\partial V_{ij}/\partial \beta_{ij} < 0$ whenever $0 < \beta_{ij} < (d_{ij}^c)^2$ and $\partial V_{ij}/\partial \beta_{ij} = 0$ whenever $\beta_{ij} \geq (d_{ij}^c)^2$.

Additionally,, W_{ij} denotes an attractive potential function between UAVs i and $j \in \mathcal{N}_i$, which is required to exhibit the following properties for aggregation.

1) W_{ij} denotes a function of squared norm of the distance between UAVs i, j, that is. not based on a vector
$$W_{ij} = W_{ij}(\|p_i - p_j\|^2) = W_{ij}(\beta_{ij}) \tag{11}$$
2) W_{ij} attains its maximum value whenever $\beta_{ij} \to \infty$. Thus, we require that $W_{ij} \to \infty$ whenever $\beta_{ij} \to \infty$.
3) It is continuously differentiable from everywhere.
4) $\partial W_{ij}/\partial p_i = 0$ and $W_{ij} = 0$ whenever $\beta_{ij} < (d_{ij}^c)^2$.
5) $\partial W_{ij}/\partial \beta_{ij} > 0$ whenever $(d_{ij}^c)^2 < \beta_{ij}$ and $\partial W_{ij}/\partial \beta_{ij} = 0$ whenever $\beta_{ij} \leq (d_{ij}^c)^2$.

Finally, the distributed formation control for each UAV i is given as the sum of the negative gradients of the two

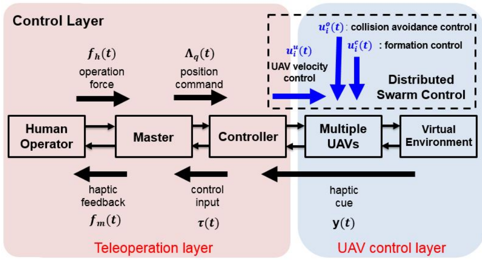

Fig. 2. Two control layers while using teleoperation

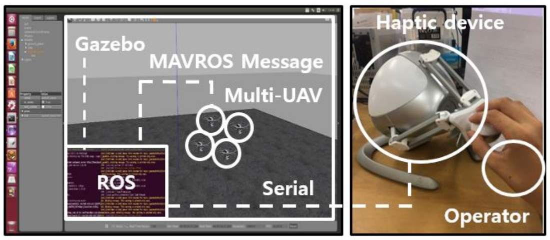

Fig. 3. Experimental Setup

potentials (10), (11) in the p_i direction: $u_i^c := -\sum_{j\in\mathcal{N}_i}\frac{\partial V_{ij}}{\partial p_i} - \sum_{j\in\mathcal{N}_i}\frac{\partial W_{ij}}{\partial p_i}$. Therefore , given the presence of two vertical asymptotes in u_i^c about the bounded potential field, the prevention of intervehicle collisions and the preservation of intervehicle connectivity is guaranteed .

3) Obstacle avoidance control u_i^o: The final velocity term, $u_i^o \in \Re^3$ c, is expressed by the following equation as a control input based on a potential field that allows multiple UAVs to avoid obstacles through a certain distance threshold: $\mathcal{D}_o \in \Re^+$

$$u_i^o := -\sum_{r\in\mathcal{O}_i}\frac{\partial\varphi_{ir}^o(\|p_i - p_r^o\|)^T}{\partial p_i} \tag{12}$$

where $\mathcal{O}_i$ denotes the set of obstacles of the ith UAV with an obstacle point p_r^o that corresponds to the position of the rth obstacle in the environment, and φ_{ir}^o denotes a certain artificial potential function that produces a repulsive action if $\|p_i - p_r^o\| < \mathcal{D}_o$, and a null action if $\|p_i - p_r^o\| \geq \mathcal{D}_o$. When the distance between the UAVs and the obstacles becomes closer to D_o, then the repulsive potential function increases to infinity.

In short, each UAV is controlled by distributed swarm control(4), and this corresponds to the sum of the three control inputs. As a result, there are two control layers that consist of a teleoperation layer, which the operator inputs control commands via the haptic device, and a UAV control layer in which a slave's motion is controlled by the distributed swarm control algorithm.

III. EVALUATION OF DISTRIBUTED SWARM CONTROL

A. Experimental Setup

The apparatus mainly consists of a desktop, a monitor that displays the simulation, and a haptic device (Fig.3). In the desktop, we used the Ubuntu14.04 LTS version of the Linux environment to simulate the virtual environment by using the Robot Operating System (ROS) and Gazebo (3D robot simulator). A virtual environment was constructed to simulate UAVs dynamics and their control laws. The dynamical control of multiple UAVs based on the distributed swarm control algorithm was simulated in a virtual environment by using Open Dynamic Engine(ODE). This environment was presented based on the Gazebo for 3D graphical rendering and on the ROS for haptic rendering, control, and communication. In the simulation, the visual scene is rendered from a camera perspective at a specific distance from the starting points of the UAVs. The graphical and haptical simulations are run at 60 Hz and 1000 Hz, respectively.

Additionally, an operator can control the virtual multi-UAV by manipulating the single haptic device. The haptic device is used as the master robot and corresponds to the commercial available Novint Falcon by Novint Technologies, Inc. with actuated linear 3-DOF and un-actuated rotational 3-DOF. It generates 3-DOF force feedback up to 8.9 N at the nominal position and its workspace is cube-shaped with an edge (4" $\times$ 4" $\times$ 4"). The device is connected to a desktop through USB with 1000 Hz servo-rate. Therefore, the desktop performs serial communication with the haptic device and communicates with the multiple UAVs through ROS messages (e.g., topics, services).

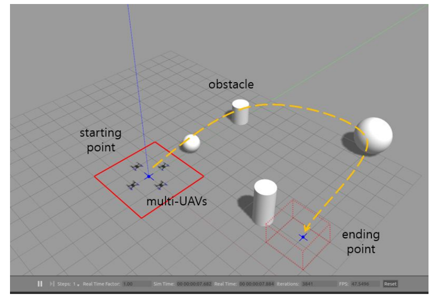

Fig. 4. Experimental Task

B. Experimental Task

The experimental task involves the flight of a multiple UAVs based on the distributed swarm control algorithm along a certain path with respect to the operator's teleoperation command (Fig.4). In the experiment, we used four UAVs to implement our goal of multiple UAV systems. During the experiment, we confirmed that multiple UAVs form the desired formation by the formation control. At this time, UAVs form a triangular pyramid with a constant relative distance. We also placed several obstacles in the path of the Task and confirmed that the UAVs avoid collisions by using the obstacle avoidance control. As shown in the Fig.4, the path is defined until UAVs arrive at the goal area from the starting point, and the experiment ends when the multi-UAVs reach the goal area.

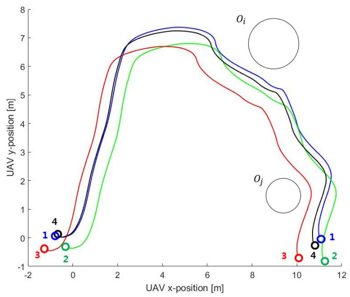

Fig. 5. Trajectory of UAVs projected on the XY planes during the task.

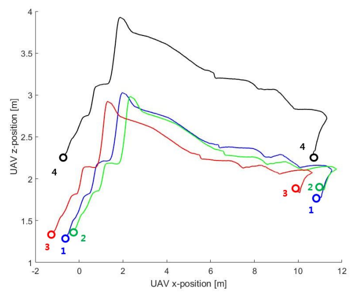

Fig. 6. Trajectory of UAVs projected on the XZ planes during the task.

C. Data Analysis

To confirm that the UAV forms well in the desired formation, avoids obstacles, and behaves in accordance with teleoperation commands, we recorded the position of the UAV(p_i), velocity of the UAV($\dot{p}_i$), position of the obstacle(p_f^o), and simulation time(ms, t) at 1000 Hz. Most of the data was sent and received via *rostopic*, and the *rosbag* was used to save the desired *rostopic*. Data analysis confirmed the following points: the multi-UAV forms a triangular pyramid shape with a constant relative distance between each other; and the UAV is automatically avoided through repulsive action based on a potential field when the distance to the obstacle is less than the distance threshold, and it should act based on the operator's desired velocity input. The results of the experiment are detailed in the following Section IV.

IV. EXPERIMENTAL RESULTS

In the experiment, a scenario was assumed wherein the operator controls the agricultural multi-UAV from the starting point to the ending point. Obstacles, such as trees and utility poles, are placed in the field (virtual world), and the agricultural task proceeds such that it passes above or beside the obstacles. The multi-UAV is assumed as a UAV for agricultural observation, spraying, or sowing. The results of the experiment obtained by using the distributed swarm control are shown in Fig.5-9.

In Fig.5-6, we present the trajectories of multiple UAVs during the experiment. This figure shows the trajectories of the UAVs controlled by the operator's teleoperation command and indicate as to whether the UAVs form the desired formation. The multi-UAV is controlled by the distributed swarm control algorithm, and the formation of the UAVs is well formed as shown in Fig.5-6. Therefore, when the multi-UAV is applied to the agriculture by using the algorithm, the operator can perform agricultural work while maintaining the desired formation of UAVs. Additionally, the operator controls via teleoperation, and thus, it is possible to work more precisely on the desired area and also to cope with an unexpected accident. Furthermore, the formation of multi-UAV is controlled by modifying the artificial potential function to form the desired formation, and it is possible to perform a flexible agricultural task by forming a one-column-array formation or a quadrilateral formation as necessary.

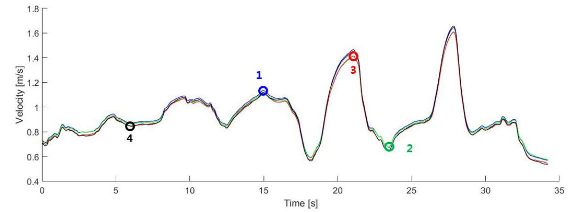

Fig. 7. Velocity of UAVs $\dot{p_i}$

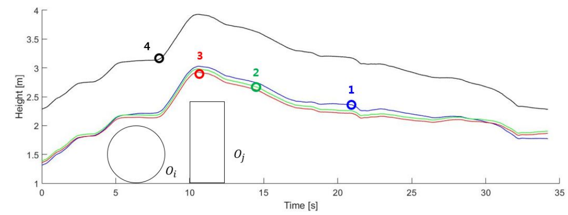

Fig. 8. Height of UAVs with Obstacles

Fig.7 shows the velocity of each UAV. In this case, the velocity control is input to each UAV as the sum of the teleoperation control of UAVs, the formation control, and the collision avoidance control. In this study, the largest input corresponds to the velocity control of teleoperation command, and the supplementary inputs correspond to the formation control and the collision avoidance control. The distributed swarm control is represented by the sum of three control inputs, and thus the formation may change based on the control input that is mainly applied. It may not be controlled as desired, and thus it is necessary to consider the most important control input . As shown in the figure, the three control inputs control each UAV via a distributed controller, and agricultural work is performed uniformly and constantly because the velocity of each UAV does not significantly differ.

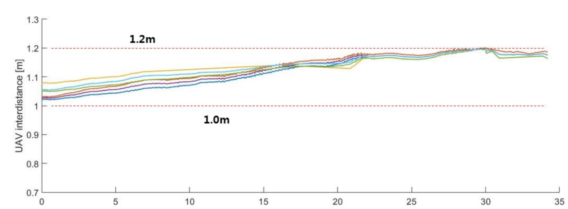

Fig. 9. Relative distance between UAVs $\|p_i - p_j\|$

Fig.8 shows the height of the UAVs and the position of the obstacles. The experimental results are mainly controlled by the collision avoidance control. In the simulation, the multi-UAV approaches upwards with respect to the first and second obstacles and approaches the side of the middle for the other two obstacles. As shown in the figure, when the distance between the UAVs and the obstacles is within a certain distance threshold, the repulsive potential field increases while approaching the obstacle, and multiple UAVs avoid the obstacles. In this manner, it is possible to avoid the increasingly frequent crashing problem caused by the collision with the utility pole when the algorithm is applied to an agricultural multi-UAV system and to safely avoid s specific obstacles when the obstacles are detected by a sensor during agricultural tasks.

Fig.9 presents the relative distances between UAVs, and the experimental results are mainly controlled by the formation control. Theoretically, it is necessary to maintain a relative distance between UAVs at a certain desired distance although it is almost impossible to implement the same. This is because position measurement errors occur at times, and the UAVs may become unstable due to disturbance, or the position of the UAVs constantly changes. Thus, it is extremely difficult to match the accurate value. Therefore, in the simulator, the relative distance between UAVs is maintained at a distance between 1 m and 1.2 m. Hence, specification of the desired range between UAVs in this manner prevents oscillation by the potential field more than that when the relative distance between UAVs is set to be a desired distance. The repulsive action was derived when the distance between the UAVs became closer to 1.0 m, and the attractive action was derived when the distance between the UAVs exceeds 1.2 m such that the formation is maintained. As shown in the figure, the distance between the UAVs does not exceed 1.2 m and is not below 1.0 m. It is assumed that a real multi-UAV system exists for agriculture. Therefore, even if multiple UAVs are used in a system when compared with a conventional system that uses a single UAV, it can be controlled stably because it maintains the desired formation while avoiding collision with others. The multiple UAVs work together, and this simultaneously increases the amount of work and the area of work, reduces the working time, and significantly increases the agricultural efficiency.

V. CONCLUSION

In this study, we proposed a distributed swarm control algorithm for agricultural multiple UAVs by using a teleoperation architecture that consisted of the following two layers: 1)a UAV control layer that controls the multiple UAVs to form a desired formation as specified by the desired distances to avoid obstacles specified by the distance threshold and to drive a specific path by UAV control method ; and 2) a teleoperation layer that controls multiple UAVs such that they move at a desired velocity given the operator's teleoperation command, and the operator simultaneously receives haptic feedback with respect to sensing UAVs and their surrounding obstacles. To apply the same to actual agricultural multi-UAV systems, we used a teleoperation method for UAV control and a distributed method for swarm control, and the methods are optimized for the agricultural environment.

ACKNOWLEDGMENT

This research was supported in part by the Basic Science Research Program through the National Research Foundation of Korea (NRF) funded by the Ministry of Science, ICT and Future Planning under Grant NRF- 2015R1C1A1A02036875, and in part by a grant (115062-2) funded by the Ministry of Agriculture, Food, and Rural Affairs (MAFRA, Korea).

REFERENCES

[1] Das, Jnaneshwar, et al. "Devices, systems, and methods for automated monitoring enabling precision agriculture." Automation Science and Engineering (CASE), 2015 IEEE International Conference on. IEEE, 2015.

[2] Katsigiannis, Panagiotis, et al. "An autonomous multi-sensor UAV system for reduced-input precision agriculture applications." Control and Automation (MED), 2016 24th Mediterranean Conference on. IEEE, 2016.

[3] Xiang, Haitao, and Lei Tian. "Development of a low-cost agricultural remote sensing system based on an autonomous unmanned aerial vehicle (UAV)." Biosystems engineering 108.2 (2011): 174-190.

[4] Doering, Dionisio, et al. "Design and optimization of a heterogeneous platform for multiple uav use in precision agriculture applications." IFAC Proceedings Volumes 47.3 (2014): 12272-12277.

[5] Jones, Chris, et al. "Principled approaches to the design of multi-robot systems." Proc. of the Workshop on Networked Robotics, IEEE/RSJ International Conference on Intelligent Robots and Systems (IROS 2004). 2004.

[6] Han, Jinlu, et al. "Low-cost multi-UAV technologies for contour mapping of nuclear radiation field." Journal of Intelligent & Robotic Systems (2013): 1-10.

[7] Chao, Haiyang, et al. "Band-reconfigurable multi-UAV-based cooperative remote sensing for real-time water management and distributed irrigation control." IFAC Proceedings Volumes 41.2 (2008): 11744-11749.

[8] Lee, Dongjun, et al. "Semiautonomous haptic teleoperation control architecture of multiple unmanned aerial vehicles." IEEE/ASME Transactions on Mechatronics 18.4 (2013): 1334-1345.

[9] Lee, Dongjun, et al. "Haptic teleoperation of multiple unmanned aerial vehicles over the internet." Robotics and automation (icra), 2011 ieee international conference on. IEEE, 2011.

[10] Franchi, Antonio, et al. "Shared control: Balancing autonomy and human assistance with a group of quadrotor UAVs." IEEE Robotics & Automation Magazine 19.3 (2012): 57-68.

[11] Borrelli, Francesco, Tams Keviczky, and Gary J. Balas. "Collision-free UAV formation flight using decentralized optimization and invariant sets." Decision and Control, 2004. CDC. 43rd IEEE Conference on. Vol. 1. IEEE, 2004.

[12] Yang, Hyunsoo, et al. "Multi-rotor drone tutorial: systems, mechanics, control and state estimation." Intelligent Service Robotics (2017): 1-15.

[13] Son, Hyoung Il, et al. "Human-centered design and evaluation of haptic cueing for teleoperation of multiple mobile robots." IEEE Transactions on Cybernetics 43.2 (2013): 597-609.

[14] Rodriguez-Seda, Erick J., et al. "Bilateral teleoperation of multiple mobile agents: Coordinated motion and collision avoidance." IEEE Transactions on Control Systems Technology 18.4 (2010): 984-992.

[15] Dimarogonas, Dimos V., and Kostas J. Kyriakopoulos. "Connectedness preserving distributed swarm aggregation for multiple kinematic robots." IEEE Transactions on Robotics 24.5 (2008): 1213-1223.